Analytical Methods

Accepted Manuscript

This is an *Accepted Manuscript*, which has been through the RSC Publishing peer review process and has been accepted for publication.

Accepted Manuscripts are published online shortly after acceptance, which is prior to technical editing, formatting and proof reading. This free service from RSC Publishing allows authors to make their results available to the community, in citable form, before publication of the edited article. This *Accepted Manuscript* will be replaced by the edited and formatted *Advance Article* as soon as this is available.

To cite this manuscript please use its permanent Digital Object Identifier (DOI®), which is identical for all formats of publication.

More information about *Accepted Manuscripts* can be found in the **Information for Authors**.

Please note that technical editing may introduce minor changes to the text and/or graphics contained in the manuscript submitted by the author(s) which may alter content, and that the standard **Terms & Conditions** and the **ethical guidelines** that apply to the journal are still applicable. In no event shall the RSC be held responsible for any errors or omissions in these *Accepted Manuscript* manuscripts or any consequences arising from the use of any information contained in them.

Graphical abstract

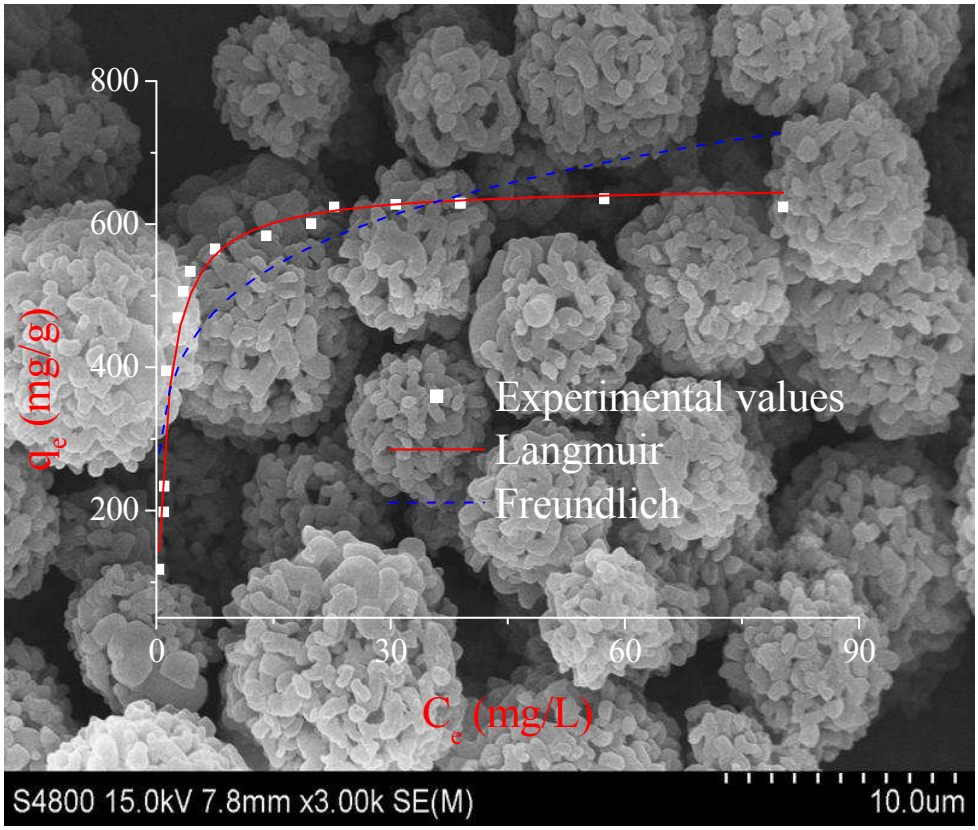

Facile synthesis of hierarchical MCM-41 spheres with ultrahigh surface area and its application for removal of methylene blue from wastewater

Qishu Qu, Zuli Gu*

College of Chemistry and Chemical Engineering, Yangzhou University, Yangzhou 225002, P. R. China

KEYWORDS: synthesis, MCM-41, hierarchical, adsorption, methylene blue.

ABSTRACT

Hierarchical mesoporous silica (HS) spheres were prepared by a simple sol-gel method and used for removing methylene blue from aqueous solutions. The macrostructure of HS can be tuned simply by adding different amount of ethanol in the reactant. The prepared HS was characterized by scanning electron microscopy, transmission electron microscopy, X-ray diffraction, nitrogen adsorption-desorption isotherm, and thermogravimetric analysis. The results showed that HS possessed both macropore and mesopore, with an average diameter of 5.6 μm, a surface area of 2280 m^2/g, and a pore volume of 1.15 cm^3/g. The influence of pH value, temperature, dosage of adsorbent, and initial MB concentration on the adsorption behavior were investigated. The experimental results showed that HS exhibited a high adsorption capacity (654.5mg/g) and extremely rapid adsorption rate (< 2 min) due to its unique hierarchical structure and very high surface area. The kinetic studies showed that experimental data were fitted well to the pseudo-first-order kinetic model. The Langmuir adsorption isotherm model was found presented an accurate description of these adsorption data. The experimental results suggest that HS is potentially useful materials for effectively adsorbing and removing of methylene blue in aqueous solution.

Introduction

Nowadays, dyes are widely used in many industrial fields such as textiles, plastics, paper, coatings, and rubber. The discharge of dyes into water has aroused people's concern because of these compounds and their degradation products can be toxic and carcinogenic.[1] In addition, a very small amount of dyes in water is highly visible leading to the visual pollution. Therefore, the development of technologies to remove dyes from wastewater is of great importance over the past decades. A variety of methods such as coagulation,[2,3] chemical oxidation,[4] membrane filtration,[5,6] photocatalytic degradation,[7-9] and adsorption[10-12] have been developed. Among all the approaches proposed, adsorption is generally preferred because of its high efficiency, easy handling, and availability of different adsorbents. The most commonly used adsorbent for dye removal was activated carbon due to its high surface area and relative high adsorption capacity.[13-15] However, commercially available activated carbons are very expensive. In addition, activated carbon suffers from slow kinetics because of the microporous structure of activated carbon. Thus, the wide application of them were restricted.[16] Therefore, many researchers have focused their efforts on developing novel adsorbents with high adsorption capacity, fast adsorption rate, and low cost.

Silica based mesoporous materials such as SBA-3,[17] SBA-15,[18-20] MCM-41,[21-24] and zeolite[25] have received much attention owing to their high surface area, large pore volume, and ordered pore structure. Both functionalized[26-28] and unfunctionalized[29] mesoporous silica can be used for dyes removal. As an efficient adsorbent, it should possess a large adsorption capacity, fast adsorption rate and easy to be separated from solution after the adsorption process. Compared to the activated carbon, the mesoporous silica provides faster adsorption rate but relatively low adsorption capacity. For example, the reported maximum adsorption capacity of activated carbon for methylene blue (MB) is 916 mg/g,[15] while the maximum adsorption capacity of mesoporous

silica for MB is only 280 mg/g.[19] The possible reason is that activated carbon possesses larger surface area and more active sites than that of mesoporous silica. However, the adsorption kinetic of mesoporous silica is fast than that of activated carbon due to the larger mean pore size of mesoporous silica. Both two kinds of adsorbent are difficult to be separated from the solution, since the sizes of these adsorbents were normally less than 1 μm. Therefore, in order to obtain an adsorbent with high adsorption capacity and fast adsorption rate, the surface area, pore size and particle size should as large as it can be.[10]

In this work, micrometer sized hierarchical mesoporous silica particles (HS) with surface area up to 2280 m^2/g were synthesized and characterized by X-ray diffraction patterns, nitrogen adsorption isotherms, thermogravimetric analysis, scanning electron microscopy, and transmission electron microscopy. A typical basic dye MB was used for testing the adsorption behavior of HS. Kinetic and equilibrium isotherm models were used to establish the rate of adsorption, adsorption capacity, and the mechanism for MB adsorption.

Experimental

Synthesis of HS

Hierarchical mesoporous silica was prepared similar as a previously reported method[30] except ethanol was used to control the particles morphology. Schematic illustration of preparation process of the HS was shown in Fig. 1. In a typical synthesis batch, 1.0 g of cetyltrimethylammonium chloride (CTAC) was dissolved in 20 mL of distilled water. Then 1 mL of ethanol, 1.48 g of sodium metasilicate ($Na_2SiO_3 \cdot 9H_2O$) and 4.8 mL of formamide ($HCONH_2$) were added at 35 ^oC with magnetic stirring, giving a clear solution. The resulting solution was stirred for 5 min at 35 ^oC and aged in a water bath for 3 h in a quiescent state. The solid product was recovered by filtration, washed with water and dried at 60 ^oC. The surfactant was removed

by calcination in air at 550 ^{o}C for 5 h. For comparison, mesoporous silica (MS) particles were prepared using the same conditions except no ethanol was added into the mixture.

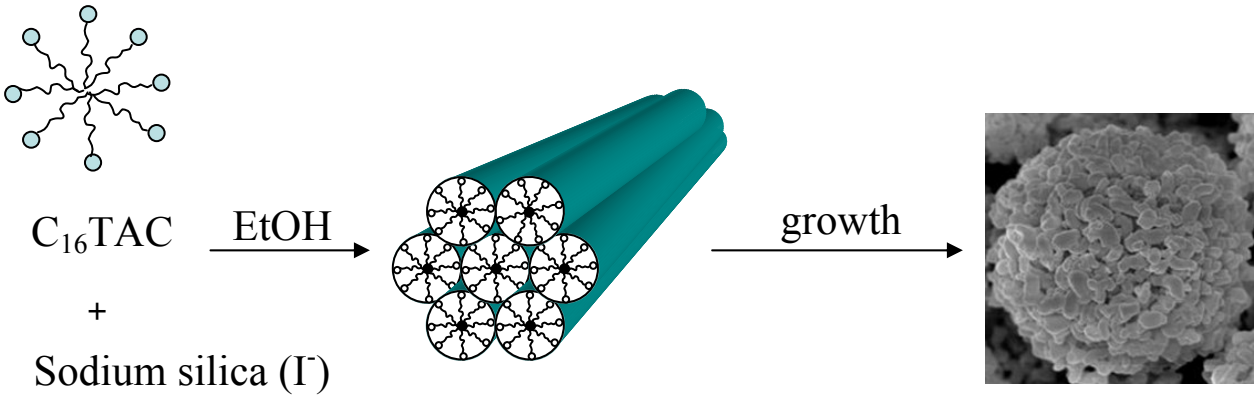

Fig. 1 Schematic illustration of preparation process of the HS.

Characterization

The morphologies of HS particles were characterized by field emission scanning electron microscopy (FESEM, Hitachi S-4800 II, 15 kV) and high-resolution TEM (HRTEM, Tecnai G2 F30 S-TWIN, 300 kV). Powder X-ray diffraction (XRD) patterns were taken on a BRUKER D8 Advance X-ray dffractometer equipped with Cu Kα radiation source. Thermogravimetric analysis (TGA) was carried out on a Pyris 1 TGA thermoanalyzer (PerkinElmer) with nitrogen as the carrier gas at a heating rate of 10 ^{o}C min^{-1}. The surface area, pore volume and pore size of the HSM particles were determined by nitrogen adsorption-desorption measurements using a Micromeritics ASAP 2010 instrument. The Brunauer-Emmett-Teller (BET) surface area was obtained by applying the BET equation to the adsorption data. The pore size distribution was

calculated from the adsorption branch of the sorption isotherms using the Barret-Joyner-Halenda (BJH) method.

Adsorption studies

Adsorption studies to evaluate the removal of MB from solutions were carried out in triplicate using a batch adsorption procedure. In a typical study, 12.5 mg of HS microspheres were added to 50 mL of MB solution with predetermined concentration. After the adsorption processes, the samples were filtered through a 0.45 μm membrane, and the filtrates were immediately determined by a UV spectrometer (Shimadzu UV-2550) at 663 nm. The equilibrium adsorption capacity of MB, q_e (mg/g) was evaluated by using the mass balance equation:

$$q_e = \frac{(C_0 - C_e) \times V}{m}$$

where C_0, C_e, V, and m are the initial and equilibrium concentrations of MB (mg/L), volume of solution (L), and mass of adsorbent (g), respectively.

The removal efficiency of adsorbents was calculated using following equation:

$$\text{removal efficiency } (\%) = \frac{C_0 - C_e}{C_0} \times 100$$

The influence of pH on the MB removal was determined by carrying out the adsorption experiments at different initial pH of the solution at 25 ^{o}C. The pH of the solution was adjusted with 0.1 M HCl or 0.1 M NaOH solutions.

The influence of temperature on the amount of MB adsorbed onto the HS was investigated under isothermal conditions in the temperature range of 25 - 65 ^{o}C in the thermostatic shaker bath.

The adsorption of MB on HS was studied by varying the amount of HS in solution (0.15 - 0.35 g/L) while keeping the initial MB concentration (30 mg/L), temperature (25 ^{o}C), and pH value (11.0).

Thermodynamic isotherm model

Two isothermal equations were used in this work to analyze the adsorption data. One is the Langmuir isotherm equation based on the assumption that adsorption on a homogeneous surface. The linear form of Langmuir isotherm equation was represented as:

$$\frac{C_e}{q_e} = \frac{1}{q_{\max} K_L} + \frac{C_e}{q_{\max}}$$

where q_{max} is the monolayer adsorption capacity (mg/g) and K_L is the Langmuir constant (L/mg).

The other isotherm equation is Freundich isotherm equation describing a heterogeneous system. The linear form of the Freundlich isotherm is as follows:

$$\ln q_e = \ln K_F + \frac{1}{n} \ln C_e$$

where K_F is the Freundlich parameter ($mg^{1-1/n}L^{1/n}/g$) and n is the heterogeneity factor, indicating the adsorption capacity and the adsorption intensity, respectively. If the values of 1/n < 1, it suggests a normal Langmuir isotherm; otherwise, it is indicative of cooperative adsorption.

Adsorption kinetics of MB

The effect of contact time on the adsorbed amount of MB was investigated at various initial concentrations of MB. Adsorption equilibrium curves were obtained at optimized pH value. Twelve point five milligrams of HS microspheres was added into a flask containing 50 mL of MB solution at 25 ^{o}C. The mixture was shaken as a function of time. At various intervals, samples were taken and residual amount of MB in the solution was determined after separation. The amount of MB adsorbed on HS particles (q_t, mg/g) at time t was calculated by the following equation:

$$q_t = \frac{(C_0 - C_t) \times V}{m}$$

where C_t (mg/L) is the concentration of MB in the solution at time t.

Kinetic models

The adsorption dynamics presented by HS were tested with the Lagergren pseudo-first-order and the chemisorption pseudo-second-order model.

The linear form of the pseudo-first-order equation is expressed as follows:

$$\log(q_e - q_t) = \log q_e - \frac{k_1}{2.303} t$$

where k_1 is the rate constant of pseudo-first-order adsorption (L/min).

The pseudo-second-order kinetic model is represented by:

$$\frac{t}{q_t} = \frac{1}{k_2 q_e^2} + \frac{1}{q_e} t$$

where k_2 is the rate constant of pseudo-second-order adsorption (g/(mg·min)).

Results and discussion

Preparation of HS

Figure 2 shows the representative SEM and HRTEM images of the mesoporous silica particles prepared using this approach. Figure 1a shows that the HS particles are formed with aggregated rod-like structures with a mean particle size of 5.6 μm. The large particle size is very helpful for the separation of these particles from the solution after the adsorption process. The HRTEM image (Fig. 2b) confirms that these spheres from the inside out were aggregated with loosely connected rods and thus formed a special interwoven macroporous structure. However, when ethanol was not used for the synthesis, mesoporous silica particles with only smooth surface were obtained (Fig. 2c,d). It suggests that the morphology of the particles is mainly affected by the amount of ethanol in the solution. The textural property of HS was further analyzed using XRD and N_2 adsorption-desorption isotherms. The XRD patterns of both HS and MS exhibited one definite peak indexed to (100) along with a broad should around 4-5 (2θ/deg) which was attributed to higher-order reflection peaks (110) and (200) (Fig. 3). These patterns are characteristic of a mesophase with a pore system lacking long-range order. Nitrogen sorption isotherms of HS shown in Fig. 4 exhibit a transitional type between type I and type IV, indicating the presence of super microporous structure.[31] The N_2 desorption isotherms of HS showed no hysteresis, suggesting that the architecture of the individual pores is uniform with no bottlenecking. The nitrogen sorption isotherms of MS however show a pronounced hysteresis

loop indicating a partial disintegration of the pore structure. As listed in Table 1, the specific surface area and the specific pore volume of MS show a marked decrease of both characteristics. Figure 5 shows the TGA traces of MS and HS. It can be found that the mass loss of surfactant from the particles amounts to ca. 40.7% of MS while that of the HS is ca. 45.3%. It indicates that the amount of surfactant required to construct the MS is less than that needed to make the HS. Therefore, it is not surprise that the surface area and pore volume of HS were larger than those of MS.

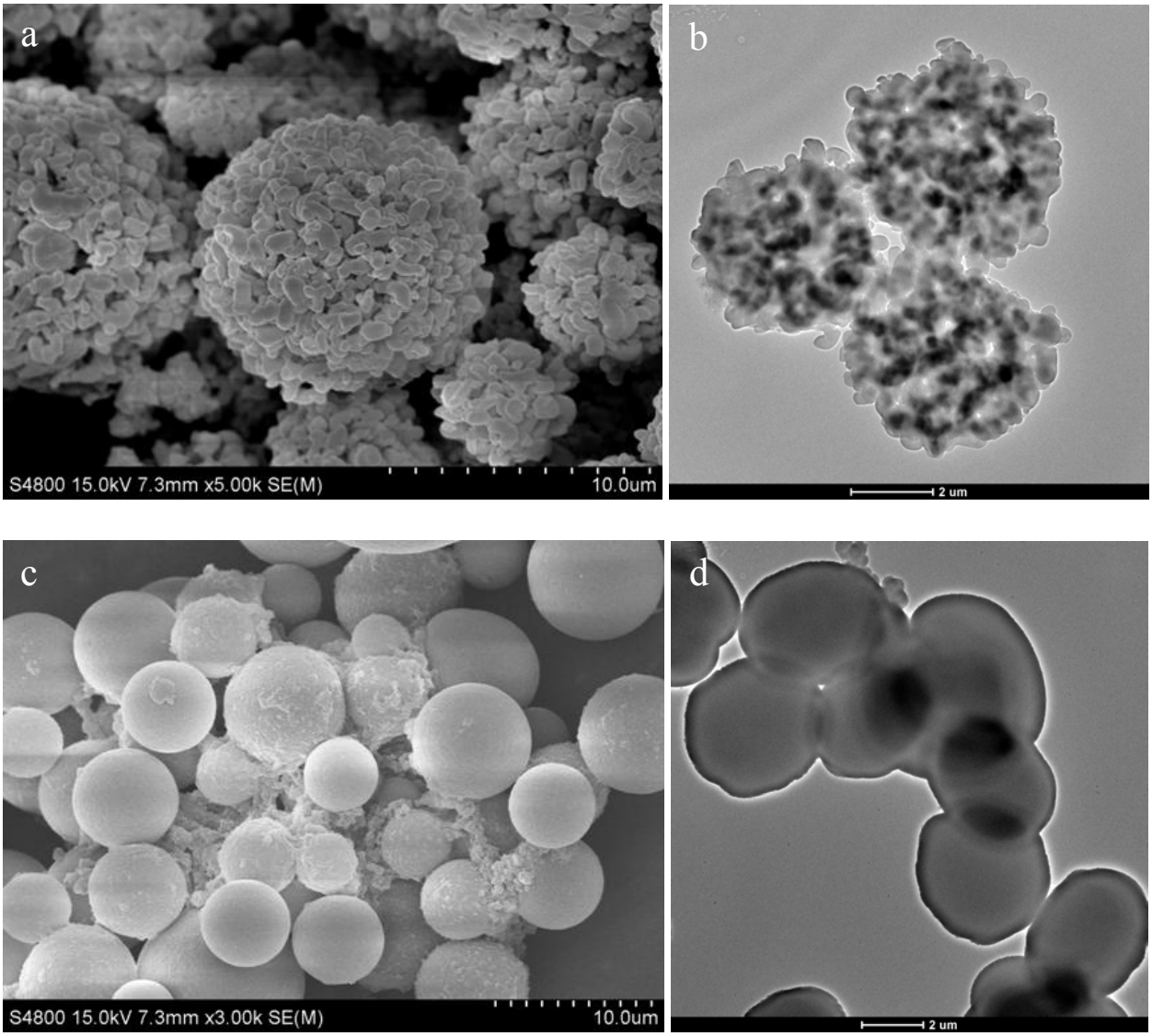

Fig. 2 SEM (a,c) and HRTEM (c,d) images of mesoporous silica particles prepared by adding 1 (a,b) and 0 mL (c,d) ethanol in the initial solution.

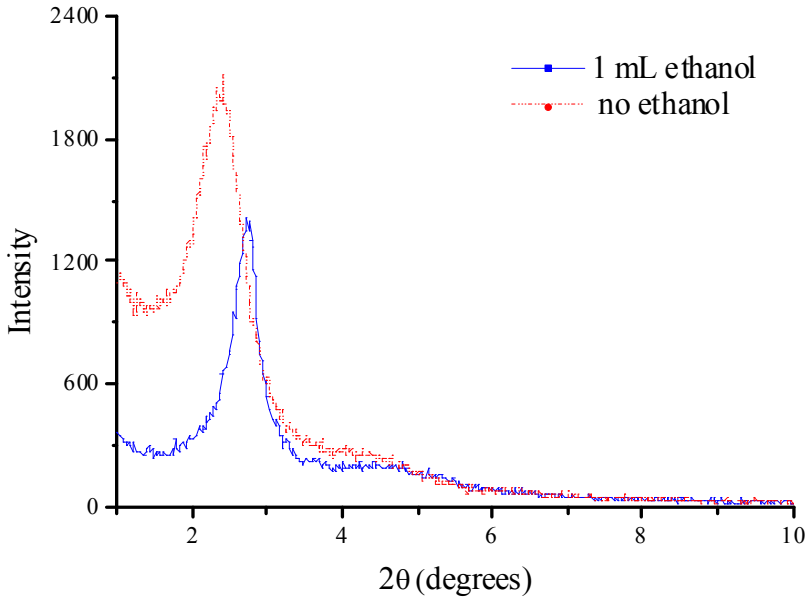

Fig. 3 XRD pattern of mesoporous silica particles obtained by adding 0 and 1 mL ethanol in the initial solution.

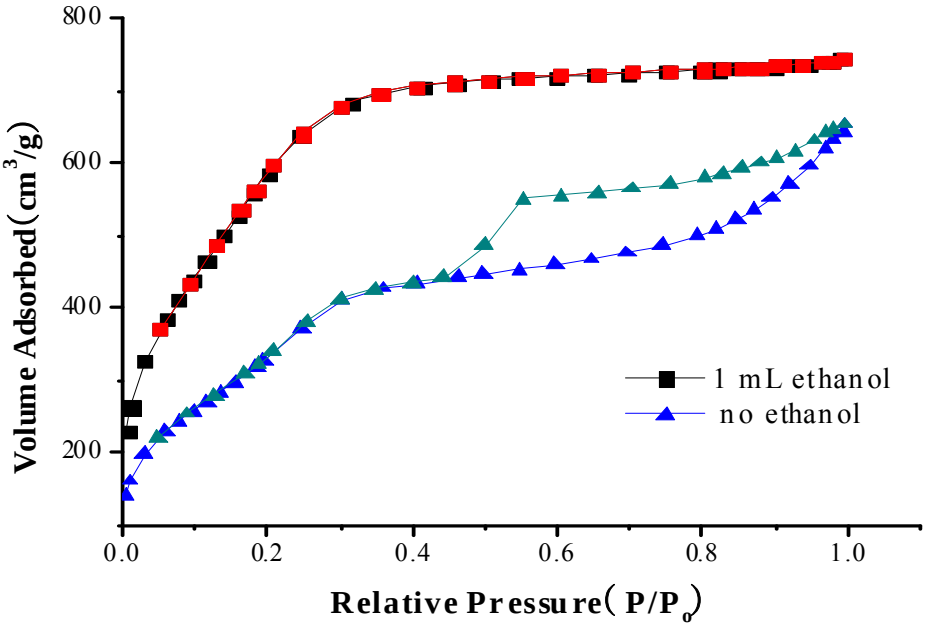

Fig. 4 Nitrogen adsorption-desorption isotherms of mesoporous silica particles obtained by adding 0 and 1 mL ethanol in the initial solution.

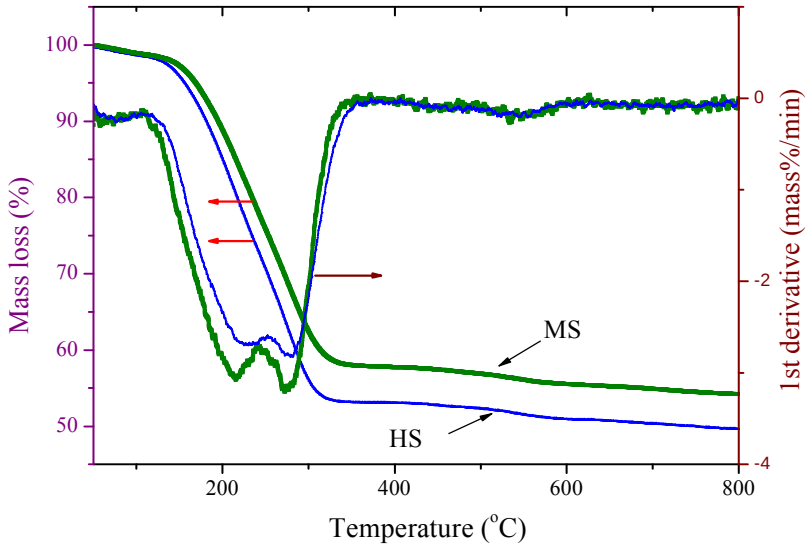

Fig. 5 Representative TG and DTG curves for mesoporous silica particles obtained by adding 0 (MS, green dot line) and 1 mL (HS, blue solid line) ethanol in the initial solution.

Table 1

Properties of MS and HS

sample	S_{BET} (m^2/g)	pore volume (cm^3/g)	pore diameter (nm)	d_{100} (nm)	mass loss (wt %)
MS	1244	0.96	3.1	4.1	40.7
HS	2280	1.15	2.0	3.5	45.3

Based on the above results, it is proposed that the particles were formed through deposition of self-assembled silicate micelles while the deposition process was mainly controlled by the

delicate competition between the rate of polymerization of silica micelles and the rate of mesostructure formation. Different deposition process leads to the formation of different morphologies. When silica source and surfactant were mixed, spherical silica/surfactant composites were soon formed through a cooperative templating mechanism[32] via an S^+I^- pathway[33]. When both the concentration of silica source and surfactant are high, the interaction between them is strong and consequently, the surfactant/silica composites grow quickly into nano-spheres. Driven by the minimum energy principle, these nano-spheres have the tendency to aggregate into big spheres in order to minimize the surface area. However, the trend of the mesostructure formation is always existent even the spherical structure is the final shape. Therefore, the attempt of these nano-spheres to elongate into a rodlike structure would become apparent when the polymerization rate decreased slightly.[34] When ethanol was added into the reactant, the solubility of $Na_2SiO_3 \cdot 9H_2O$ decreased which makes the interaction between the silica source and surfactant decreased. Thus, silica spheres composed with small rodlike submicrometer particles were obtained. In addition, the existence of ethanol could disrupt the self-assembly of surfactant micelles due to the decrease of the surfactant aggregates for the weak solvophobic effect.[35] Therefore, the amount of surfactant incorporated in the formation of silica/surfactant composites decreased which is in line with the results of thermogravimetry analysis (Fig. 5). When the volume of ethanol was further increased to 2 mL, only hexagonal or hexagonal-like silica rods were obtained (Supplementary Information, Fig. S1-4). These experimental results confirmed our proposal.

Due to the hierarchical structure of HS, BET surface area as high as 2280 m^2/g was obtained. The existence of the macropores in HS makes the mass transfer between adsorbate and adsorbent becoming easy. Furthermore, the existence of the marcropores helped to expose more inner surface area to the adsorbate, which could provide more Si-OH groups used as active adsorption

site. Thus, this kind of particle is expected to be a promising adsorbent for removal of dyes or metal ions from the wastewater.

Adsorption behaviours of the HS

Effect of pH

The pH of dye solution plays an important role in the whole adsorption process. It affects the degree of ionization of the adsorbent and the adsorbate thereby altering the reaction kinetics and equilibrium characteristics of adsorption process. MB is a cationic dye. In aqueous solution it exists in form of positively charged ions.[36] The pKa of the silica is about 1.5.[37] Therefore, the silica particles are negatively charged and the cationic groups increased with increasing pH value. Meanwhile, with the pH value increased, the competition of H^+ with positively charged MB cations decreased. As a result, the adsorption capacity increased with increasing pH value from 6 to 10 as that shown in Fig. 6. When pH value further increased from 10 to 11, silica and MB were fully ionized. Thus, the adsorption capacity remained steady.

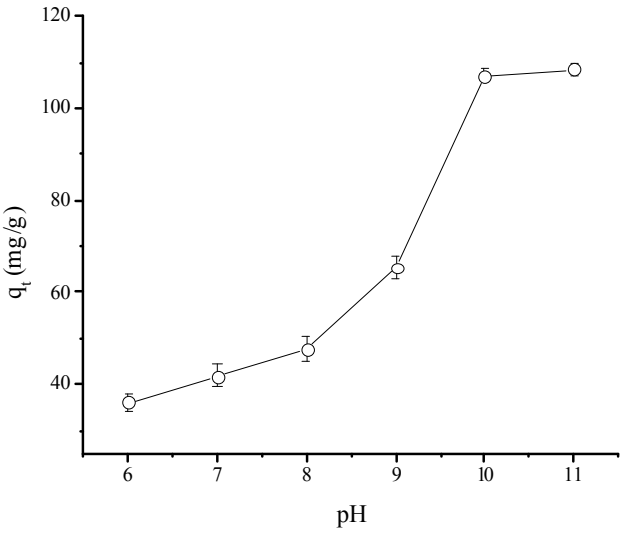

Fig. 6 Effect of initial pH on the removal of methylene blue (C_0, 30 mg/L; adsorbent dosage, 0.25 g/L; temperature, 25 ^oC; contact time, 15 min).

Effect of temperature

The effect of temperature on the adsorption capacity reflects the thermodynamics of MB removal on the HS. It can be seen from the Fig. 7 that there is a slight decrease in adsorption capacity as temperature increased from 25 to 45 ^oC, while a more significant decrease was obtained over the temperature range 45 to 65 ^oC. These experimental results suggest that the adsorption and desorption rate between HS and MB was very quickly while the former one is larger than the latter when the temperature is low. However, with the temperature increases, the enhancement of the desorption rate was bigger than that of adsorption rate. So the adsorption capacity decreased with decreasing temperature. The fast adsorption rate of HS at low temperature is owing to its unique hierarchical structure which makes the mass transfer easily.

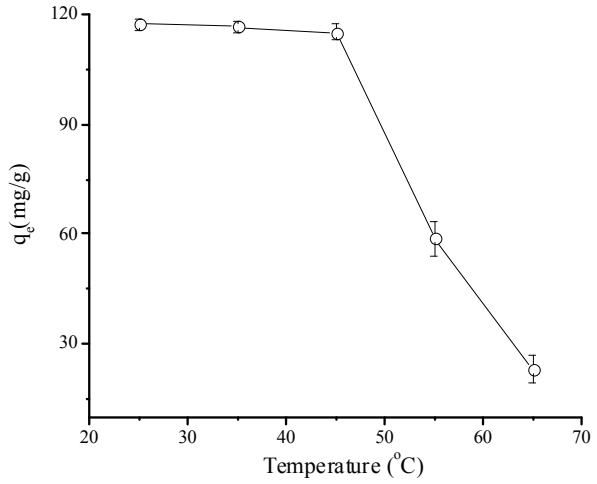

Fig. 7 Effect of temperature on the removal of methylene blue (C_0, 30 mg/L; adsorbent dosage, 0.25 g/L; temperature, 25 ^oC; pH 11.0).

Effect of Adsorbent Dosage

The adsorption of MB onto HS was studied by varying the HS concentration (0.15 – 0.35 g/L) while keeping the initial MB concentration, temperature, pH value, and contact time constant. As that shown in Fig. 8, the adsorption capacity decreased with increasing amount of adsorbent, whereas, the removal efficiency increased as the adsorbent concentration increased. The increase in MB removal with increasing adsorbent mass can be attributed to the increase in the total surface area. However, the decreased adsorption capacity indicates that adding too many adsorbent in the solution is wasteful, since the removal efficiency only increased a little (96.1% - 98.5%) when the adsorbent concentration increased from 0.15 to 0.35 g/L. Considering that in the industrial process more adsorbents were used to make sure that all the dyes in the wastewater could be removed, in our case, the adsorbent concentration was fixed at 0.25 g/L.

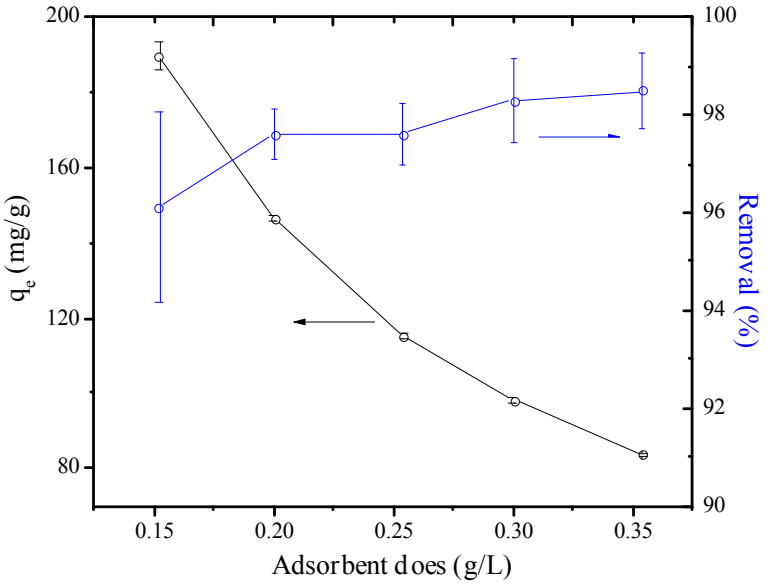

Fig. 8 Effect of adsorbent dosage on the adsorption capacity and removal efficiency of MB (C_0, 30 mg/L; temperature, 25 ^oC; contact time, 15 min; pH 11).

Kinetic studies

In order to investigate the mechanism of adsorption and potential rate controlling steps, kinetic studies were carried out for different contact time at different initial MB concentrations. It appears from Fig. 8 that, for all concentrations of MB, the adsorption equilibrium could be achieved within 2 minutes and no significant change was observed from 2 to ca. 40 min, which suggests the rate of uptake of MB is considerably fast.

Pseudo-first-order model is based on the hypothesis that the rate of occupation of the adsorption sites proportional to the number of unoccupied sites, while the pseudo-second-order model is assumed that the adsorption rate is controlled by chemical adsorption through sharing or exchange of electrons between the adsorbent and adsorbrate.[18] Parameters of two kinetic models are given in Table 2. As can be seen in Table 2, the correlation coefficients calculated from both two kinetic models were very high (> 0.9996) for all MB concentrations, and the theoretical ($q_{e,cal}$) value calculated from the pseudo-first-order model agreed well with the experimental ($q_{e,exp}$) values. Therefore, the adsorption process of MB on the HS is mainly a physical process. However, this result is different with the results reported before that pseudo-second-order model is more suitable for describing the similar adsorption process[17,18,20] when mesoporous silica was used as adsorbent. This difference can be attributed to the hierarchical structure of HS leads to a faster adsorption process rate than other silica based mesoporous materials. So the adsorption could be finished at the initial stage of adsorption, being fitted well by pseudo-first-order model. The same phenomenon was obtained by using hierarchical activated carbon[14] or marcoporous silica gel as adsorbents[38] for the adsorption of MB.

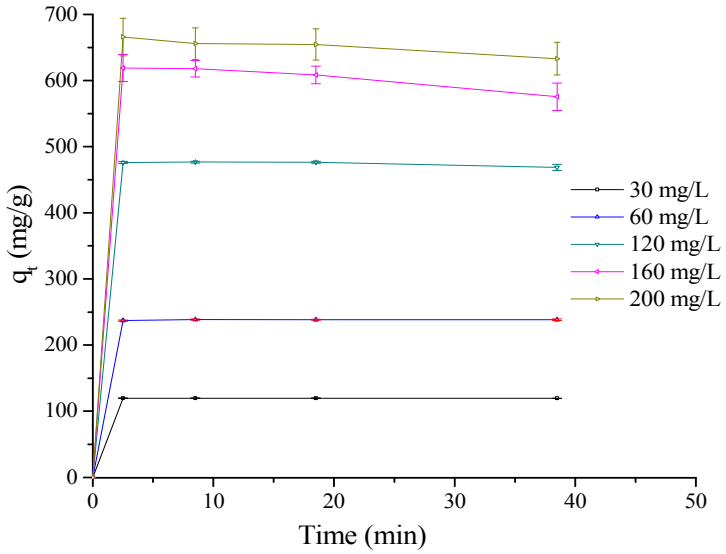

Fig. 9 Effect of initial concentration of MB on the adsorption rate (adsorbent dosage, 0.25 g/L; temperature, 25 ^{o}C; pH 11, MB concentrations were in the range of 30-240 mg/mL).

Table 2

Pseudo-first-order and pseudo-second-order kinetics parameters for the adsorption of MB onto HS

C_0 (mg/L)	$q_{e,exp}$ (mg/g)	pseudo-first-order model			pseudo-second-order model		
		k_1 (min^{-1})	$q_{e,cal}$ (mg/g)	R^2	k_2 (g mg^{-1} min^{-1})	$q_{e,cal}$ (mg/g)	R^2
30	119.6	23.22	119.6	0.9999	0.0225	120.8	0.9999
60	237.9	2.233	237.9	0.9999	0.1167	239.2	0.9999

120	476.7	36.42	474.5	0.9997	0.0446	480.8	0.9999
160	619.0	425.8	605.5	0.9996	0.0088	632.9	0.9998
200	665.9	306.6	652.3	0.9998	0.0083	675.7	0.9998

Adsorption isotherms

The adsorption isotherms describe the distribution of adsorbate between the liquid phase and solid phase when the system reaches the equilibrium.[39] As shown in Fig. 10, HS has a large adsorption capacity for MB. The saturation adsorption capacity of HS to MB is 654.5 mg/g, which is much larger than those of the same dye onto most conventional silica based mesoporous materials as that shown in Table 3. The adsorption equilibrium data were fitted to the Langmuir and Freundlich isotherms. The parameters and correlation coefficients calculated from the models are listed in Table 4. It can be seen that the least-squares correlation coefficient (R^2) values of Langmuir model is significantly higher than that of Freundlich model for MB removal, indicating that Langmuir model should better describe the MB adsorption onto the HS.

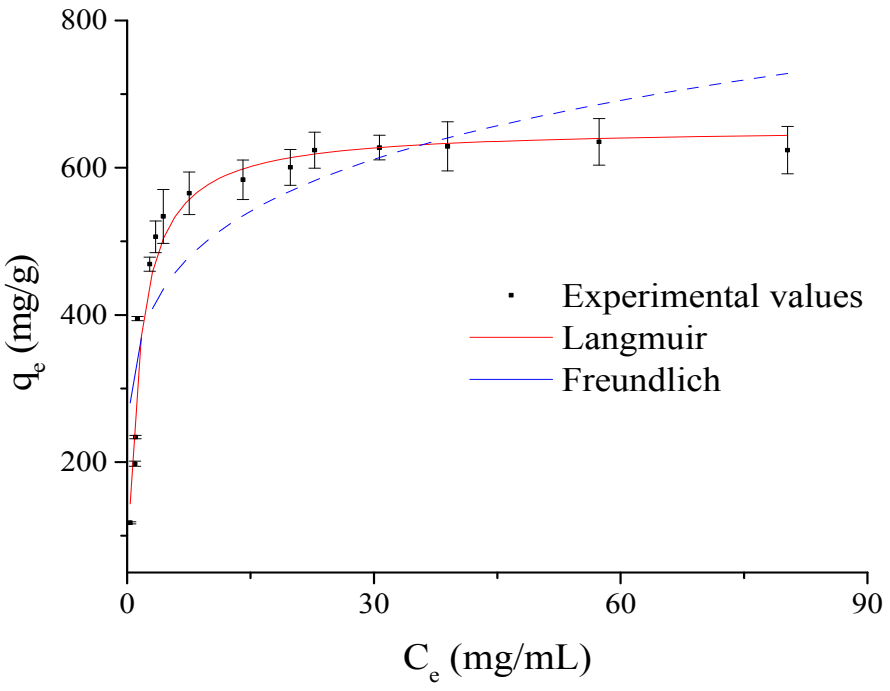

Fig. 10 Nonlinear fits of isotherm models of Langmuir and Freundlich (adsorbent dosage, 0.25 g/L; temperature, 25 ^{o}C; pH 11).

Table 3

Comparison of the maximum monolayer adsorption capacity of MB on various silica based adsorbents

adsorbent	maximum adsorption capacity (mg/g)	reference
silsesquioxane functionalized Silica gel	54	40
silica nano-sheets	11.8	41
carboxylate functionalized SBA-15	159	27
SBA-15	49.3	18

multicarboxylic hyperbranched polyglycerol functionalized SBA-15	160	20
amino functionalized MCM-41	54	21
SBA-15	280	19
SBA-3	ca. 284	17
MCM-41	654.5	this work

Table 4

Parameters of adsorption isotherms of MB onto HS

isotherms	parameters	value
Langmuir model	q_{max} (mg/g)	654.5
	K_L (L/mg)	0.7583
	R^2	0.9566
Freundlich model	K_F ($mg^{1-1/n}L^{1/n}/g$)	334.7
	1/n	0.1772
	R^2	0.7501

Conclusions

Mesoporous silica particles with hierarchical structure were synthesized by using ethanol as cosurfactant. The present study shows that thus prepared hierarchical mesoporous silica particles are efficient adsorbent for the removal of methylene blue from aqueous solution. The adsorption rate is very fast and adsorption equilibrium could be reached in 2 min. The adsorption isotherms can be well fitted with Langmuir model, showing a maximum monolayer adsorption capacity of 654.5 mg/g. The adsorption process follows the pseudo-first-order model, which suggests that the process was controlled by physisorption.

Acknowledgements

This work was supported by NSFC (20975090).

Notes and references

1 M. T. Uddin, M. A. Islam, S. Mahmud and M. Rukanuzzaman, *J. Hazard. Mater.*, 1999, **164** 53.

2 P. Cañizares, F. Martínez, C. Jiménez and J. Lobato, *Environ. Sci. Technol.*, 2006, **40**, 6418.

3 B. Y. Shi, G. H. Li, D. S. Wang, C. H. Feng and H. X. Tang, *J. Hazard.Mater.*, 2007, **143**, 567.

4 G. S.Wu, J. P. Wang, D. F. Thomas and A. C. Chen, *Langmuir*, 2008, **24**, 3503.

5 R. S. Juang and R. C. Shiau, *J. Membr. Sci.*, 2000, **165**, 159.

6 J. W. Lee, S. P. Choi, R. Thiruvenkatachari, W. G. Shim and H. Moon, *Water Res.*, 2006, **40**, 435.

7 M. Muruganandham and M. Swaminathan, *J. Hazard. Mater.*, 2006, **135**, 78.

8 T. H. Liou and B. C. Lai, *Appl. Catal. B: Environ.*, 2012, **115-116**, 138.

9 H. Y. Jiang, X. Meng, H. X. Dai, J. G. Deng, Y. X. Liu, L. Zhang, Z. X. Zhao and R. Z. Zhang, *J. Hazard. Mater.*, 2012, **217-218**, 92.

10 W. P. Shi, S. Y. Tao, Y. X. Yu, Y. C. Wang and W. Ma, *J. Mater. Chem.*, 2011, **21**, 15567.

11 D. Mahanta, G. Madras, S. Radhakrishnan and S. Patil, *J. Phys. Chem. B*, 2008, **112**, 10153.

12 M. Anbia, S. A. Hariri and S. N. Ashrafizadeh, *Appl. Surf. Sci.*, 2010, **256**, 3228.

13 J. T. Li, B. L. Li, H. C. Wang, X. B. Bian and X. M. Wang, *Carbon*, 2011, **49**, 1912.

14 X. Z. Yuan, X. S. Shi, S. J. Zeng and Y. L. Wei, *J. Chem. Technol. Biotechnol.*, 2011, **86**, 361.

15 A. L. Cazetta, A. M. M. Vargas, E. M. Nogami, M. H. Kunita, M. R. Guiherme, A. C. Martins, T. L. Silva, J. C. G. Moraes and V. C. Almeida, *Chem. Eng. J.*, 2011, **174**, 117.

16 I. Ali and V. K. Gupta, *Nat. Protoc.*, 2007, **1**, 2661.

17 M. Anbia and S. A. Hariri, *Desalination*, 2010, **261**, 61.

18 C. H. Huang, K. P. Chang, H. D. Ou, Y. C. Chiang and C.F. Wang, *Micropor. Mesorpor. Mater.*, 2011, **141**, 102-109.

19 Y. L. Dong, B. Lu, S. Y. Zang, J. X. Zhao, X. G. Wang and Q. H. Cai, *J. Chem. Technol. Biotechnol.*, 2011, **86**, 616.

20 Z. J. Chen, L. Zhou, F. A. Zhang, C. B. Yu and Z. B. Wei, *Appl. Surf. Sci.*, 2012, 258, 5291.

21 K. Y. Ho, G. McKay and K. L. Yeung, *Langmuir*, 2003, **19**, 3019.

22 L. C. Juang, C. C. Wang and C. K. Lee, *Chemosphere*, 2006, **64**, 1920.

23 Q. D. Qiu, J. Ma and K. Liu, *J. Hazard. Mater.*, 2009, **162**, 133.

24 P. Monash and G. Pugazhenthi, *Korean J. Chem. Eng.*, 2010, **27**, 1184.

25 W.T. Tsai, K. J. Hsien, H. C. Hsu, *J. Hazard. Mater.*, 2009, **166**, 635.

26 Z. Yan, G. T. Li, L. Mu and S. Y. Tao, *J. Mater. Chem.*, 2006, **16**, 1717.

27 Z. Yan, S. Y. Tao, J. X. Yin and G. T. Li, *J. Mater. Chem.*, 2006, **16**, 2347.

28 X. C. Fu, X. Chen, J. Wang and J. H. Liu, *Micropor. Mesopor. Mater.*, 2011, **139**, 8.

29 S. B. Wang, H. T. Li and L. Y. Xu, *J. Colloid Interface Sci.*, 2006, **295**, 71.

30 S. P. Naik and, I. Sokolov, *Solid State Commun.*, 2007, **144**, 437.

31 M. Casagrande, L. Storaro, M. Lenarda, J. Gersich, L. Stievano, F. E. Wagner and T. Montanari, *J. Mater. Chem.*, 2004, **14**, 1010.

32 A. Firouzi, D. Kumar, L. M. Bull, T. Besier, P. Sieger, Q. S. Huo, S. A. Walker, J. A. Zasadzinski, C. Glinka, J. Nicol, D. Margolese, G. D. Stucky and B. F. Chmelka, *Science*, 1995, **267**, 1138.

33 Q. S. Huo, D. I. Margolese, U. Ciesla, P. Y. Feng, T. E. Gier, P. Sieger, R. Leon, P. M. Peroff, F. Schüth and G. D. Stucky, *Nature*, 1994, **368**, 317.

34 I. Beurroies, P. Ågren, G. Büchel, J. B. Rosenholm, H. Amenitsc, R. Denoyel and M. Linden, *J. Phys. Chem. B*, 2006, **110**, 16254.

35 S. Q. Liu, P. Cool, O. Collart, P. Van Der Voort, E. F. Vansant, O. I. Lebedev, G. V. Tendeloo and M. H. Jiang, *J. Phys. Chem. B*, 2003, **107**, 10405.

36 J. Q. Xue, W. B. Mao, Y. J. Wang, J. X. Li and M. Wu, *Rare Metals*, 2011, **30**, 249.

37 B. C. Lin, Introduction to Capillary Electrophoresis, Science Press, Beijing 1996, p. 9.

38 G. Q. Liu, R. Yang and M. Li, *J. Non-Cryst. Solids*, 2010, **356**, 250.

39 J. M. Gong, T. Liu, X. Q. Wang, X. L. Hu and L. Z. Zhang, *Environ. Sci. Technol.*, 2011, **45**, 6181.

40 D. S. F. Gay, T. H. M. Fernandes, C. V. Amavisca, N. F. Cardoso, E. V. Benvenutti, T. M. H. Costa and E. C. Lima, *Desalination*, 2010, **258**, 128.

41 M. F. Zhao, Z. B. Tang and P. Liu, *J. Hazard. Mater.*, 2008, **158**, 43.